

02.80.05

REPRINT

RADIOCHEM. RADIOANAL. LETTERS 43/5/ 265-278 /1980/

EXCITATION FUNCTIONS AND THICK TARGET YIELDS OF
 $/\alpha, xn/$ AND $/\alpha, \alpha xn/$ REACTIONS ON ^{103}Rh

M.J. Ozafran, M.E. Vazquez, M. De la Vega Vedoya,
S.J. Nassiff

Comision Nacional de Energia Atomica, Argentina

Received 12 March 1980

Accepted 22 March 1980

C. N. E. A. Biblioteca	
ARCHIVO PUBLICACIONES	
NO 1	AÑO 1980

EXCITATION FUNCTIONS AND THICK TARGET YIELDS OF
 $[\alpha, xn]$ AND $[\alpha, \alpha xn]$ REACTIONS ON ^{103}Rh

M.J. Ozafran, M.E. Vazquez, M. De la Vega Vedoya,
S.J. Nassiff

Comision Nacional de Energia Atomica, Argentina

Received 12 March 1980

Accepted 22 March 1980

Excitation functions were determined by the "stacked foil" method at the Buenos Aires 60 inch Synchrocyclotron for the $[\alpha, xn]$ and $[\alpha, \alpha xn]$ reactions on ^{103}Rh , up to 55 MeV. Thick-target yields were calculated as a function of energy for the production of ^{105}Ag and $^{106\text{m}}\text{Ag}$.

INTRODUCTION

The experimental information available on α -reaction cross-sections has until now been very scarce.

During the last decade, considerable progress was achieved in techniques for the counting and absolute standardization of radioactivity, as well as in the quality of charged particle beams. Therefore, excitation functions determined at present by use of the "stacked-foil" method should yield in more accurate and reproducible measurements.

Early work on $[\alpha, n]$ and $[\alpha, 2n]$ reactions of ^{103}Rh was done by Bradt et al.¹ in 1947. In all these measurements, done by activation, no absolute cross-sections were obtained.

In the present work absolute $\sigma/\alpha, xn/$ and $\sigma/\alpha, \alpha xn/$ on ^{103}Rh have been measured up to 55 MeV using a solid state detector /Ge intrinsic/.

EXPERIMENTAL

Irradiations

The experiments were performed in a similar way to that outlined in previous papers²⁻⁶. Stacks of rhodium foils /17.70 mg/cm²/ were irradiated in the external beam of the 60 inch Synchrocyclotron of Buenos Aires. Maximum uncertainty in the incident beam energy was estimated as being lower than 1%. The rhodium and copper foils were analyzed spectroscopically for interfering impurities; the amount of these were found to be negligible.

The stack consisted of target foils inserted between appropriately chosen catcher foils of copper to collect the recoils escaping from the targets, and also copper absorbers which degraded the energy of the bombarding particles. Furthermore, in order to estimate the contribution of reaction products induced by fast and slow neutrons on target material, target and catcher foils were stacked well beyond the range of 55 MeV α -particles.

The copper foils were also used for the determination of the excitation function of the reaction $^{65}\text{Cu}/\alpha, 2n/^{67}\text{Ga}$ needed for the monitoring of the ion current. The cross-section values established by Porile et al.⁷ were taken as standards.

The mean α -particle energy for each foil was calculated by means of a computer program⁸ based on the range energy relationships given in the literature⁹.

The uncertainty of the incident energy was estimated to be below 1%, while fluctuations in the primary beam energy during bombardment were calculated to be less than 0.3 MeV. Within the straggling in energy losses in the foils, effective energy spreads of 0.5 MeV were obtained for 10 MeV α -particles.

A comparison of the yields of the radioactive isotopes formed in the irradiation of rhodium with that of ^{67}Ga yield in copper foils permits to obtain the absolute cross-section values for the concerned reactions resulting of rhodium with α -particles.

•

Counting

The cross-sections were measured by the activation method.

Since the determination of the reaction products was done by the non-destructive procedure on target and monitoring foils, possible errors introduced by chemical treatment and special source preparation were avoided.

After bombardment, the γ -spectra of each sample were measured using a high resolution Ge intrinsec detector coupled to a multichannel pulse-height analyzer.

The nuclides produced by α -induced reactions, were recognized following carefully the decay curves at each photopeak energy.

The photopeak areas were calculated by using Wasson's method^{10,11} with a HUNTER program¹².

Standard sources of γ -emitters with well-known values of energy and intensities of γ -rays were used for the accurate calibration of the energy and detection efficiency of the spectrometer. Most efficiency determinations agreed with the statistical error of 3%. The formula

$\epsilon/E_Y/ = \text{const. } E_Y^{-n}$ was used to interpolate the efficiency $\epsilon/E_Y/$ to other energies. A computer program was developed¹³.

The areas of all γ -peaks observed were corrected for efficiency of detection and the activities of the radioactive products were calculated separately for each peak on the basis of the nuclear data^{14,15}.

Foil thicknesses and α -particles flux were measured and used to calculate cross-sections for the active isotopes found in each foil. Corrections for the energy spread in each foil due to uncertainties in the foil thickness and the energy decrease in the preceding foils were not applied. Losses of reaction products by recoil were assumed to be negligible.

Spectra from those foils set up beyond the range of α -particles that might belong to secondary neutrons showed no significant contribution to our data.

RESULTS AND DISCUSSION

The cross-sections and excitation functions for the reactions measured in the present work are given in Tables 1 and 2 and Figs 1 to 6. In Fig. 1 our results are compared with those of Hansen and Stelts¹⁶.

Threshold energies given by Keller, Lange and Münzel¹⁷ are shown on the respective graphs.

Uncertainties in the cross-section values were estimated by propagating in quadrature the contributions from both, decay curve and peak analysis /the latter including statistics/, absolute detector efficiencies, disintegratic schemes, target thicknesses and deuteron flux.

The excitation functions may in some instances include contributions from the decay of short life precursors.

TABLE 1

Cross-sections for the $/\alpha, n/$ and $/\alpha, 2n/$ reactions on ^{103}Rh

E_α /MeV/	σ /mb/			
	$^{103}\text{Rh}/\alpha, n/$	$^{106\text{m}}\text{Ag}$	$^{103}\text{Rh}/\alpha, 2n/$	$^{105\text{g}}\text{Ag}$
54.3	6.8	+ 4.1	34.7	+ 2.6
51.4	7.9	+ 4.0	49.9	+ 4.2
48.5	5.8	+ 7.4	58.2	+ 5.0
45.6	-		99.5	+ 6.2
40.6	8.1	+ 4.4	103.4	+ 8.1
39.0	13.3	+ 6.6	129.6	+ 9.8
37.3	14.3	+ 7.1	169.3	+ 12.8
33.5	33.3	+ 19.3	346.8	+ 26.3
31.6	51.13	+ 26.4	423.5	+ 34.8
29.6	66.9	+ 33.3	693.3	+ 52.3
24.6	80.9	+ 40.3	757.4	+ 57.3
22.2	79.0	+ 39.3	617.6	+ 46.7
19.7	31.5	+ 15.7	397.7	+ 30.13
16.9	14.1	+ 7.2	16.48	+ 1.2
10.1	10.1	+ 5.1		

$^{105\text{g}}\text{Ag}$, $^{104\text{g}}\text{Ag}$ and $^{103\text{g}}\text{Ag}$ directly produced by $^{103}\text{Rh}/\alpha, 2n/^{103}\text{Ag}$, $^{103}\text{Rh}/\alpha, 3n/^{104}\text{Ag}$ and $^{103}\text{Rh}/\alpha, 4n/^{103\text{g}}\text{Ag}$, would be partially generated by $^{105\text{m}}\text{Ag}$, $^{104\text{m}}\text{Ag}$ and $^{103\text{m}}\text{Ag}$, respectively, and therefore they would contribute to the measured yields of $^{105\text{g}}\text{Ag}$, $^{104\text{g}}\text{Ag}$ and $^{103\text{g}}\text{Ag}$.

The maximum cross-section values obtained from our data were compared with systematics for excitation functions^{17,18}. A good agreement was found.

Within the frame of this work, no attempt was made to clarify the reaction mechanisms involved with the excitation functions we report on work.

TABLE 2
 Cross-sections for the $/\alpha,3n/$, $/\alpha,4n/$, $/\alpha,\alpha3n/$ and $/\alpha,\alpha4n/$ reactions on ^{103}Rh

E_α /MeV/	σ /mb/					
	$^{103}\text{Rh}/\alpha,3n/^{1049}\text{Ag}$	$^{103}\text{Rh}/\alpha,4n/^{1039}\text{Ag}$	$^{103}\text{Rh}/\alpha,\alpha3n/^{100}\text{Rh}$	$^{103}\text{Rh}/\alpha,\alpha4n/^{99\text{m}}\text{Rh}$		
54.3	-	632.7 ± 31.6	35.7 ± 5.1	19.7 ± 4.7		
48.3	255.9 ± 10.9	-	40.8 ± 6.1	13.2 ± 4.0		
46.8	273.2 ± 11.7	530.5 ± 25.0	54.2 ± 4.7	11.48 ± 4.0		
43.4	497.46 ± 21.4	564.6 ± 26.5	67.8 ± 4.0	8.1 ± 5.8		
41.8	613.0 ± 26.5	358.13 ± 17.7	79.60 ± 4.8	-		
38.6	700.7 ± 30.3	292.4 ± 16.0	97.6 ± 4.6	3.3 ± 4.2		
36.8	703.3 ± 30.6	124.2 ± 15.2	73.5 ± 4.3	-		
31.2	476.1 ± 20.9	-	-	-		
27.0	261.4 ± 11.6	-	46.8 ± 4.1	-		
24.8	108.7 ± 4.9	-	8.8 ± 1.4	-		

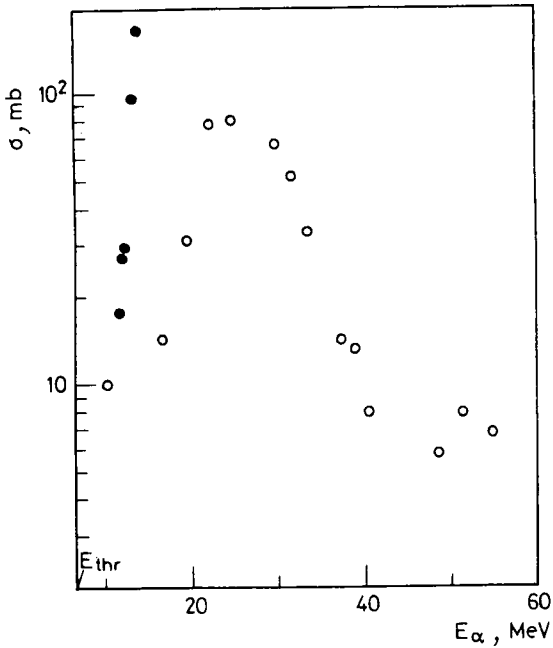


Fig. 1. Excitation function for the $^{103}\text{Rh}/\alpha, n/^{106\text{m}}\text{Ag}$ reaction. ooooo Our results; ●●●●● Ref. 16

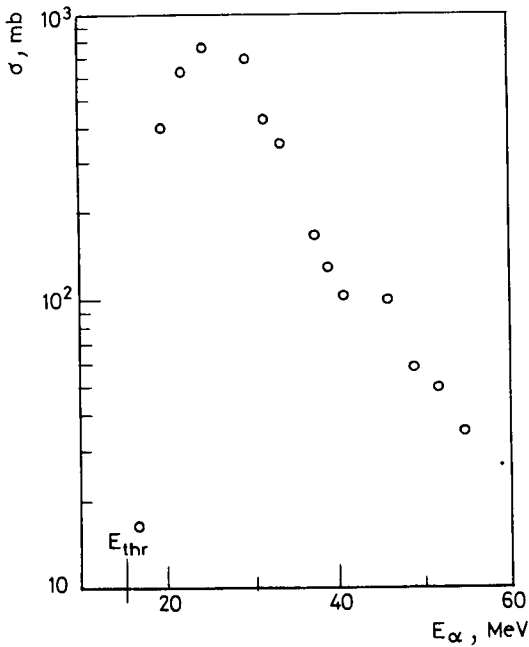


Fig. 2. Excitation function for the $^{103}\text{Rh}/\alpha, 2n/^{105\text{g}}\text{Ag}$ reaction

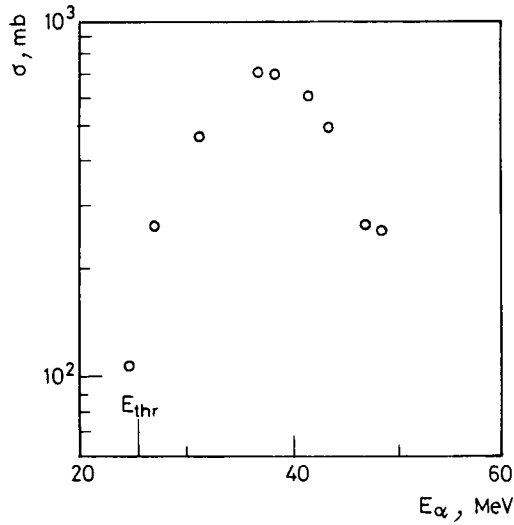


Fig. 3. Excitation function for the $^{103}\text{Rh}/\alpha, 3n/^{104g}\text{Ag}$ reaction

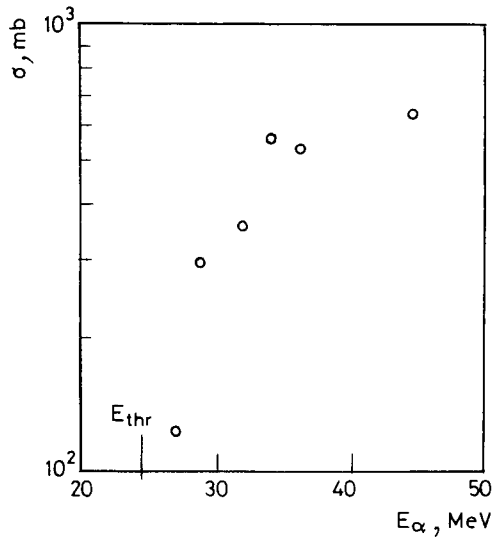


Fig. 4. Excitation function for the $^{103}\text{Rh}/\alpha, 4n/^{103g}\text{Ag}$ reaction

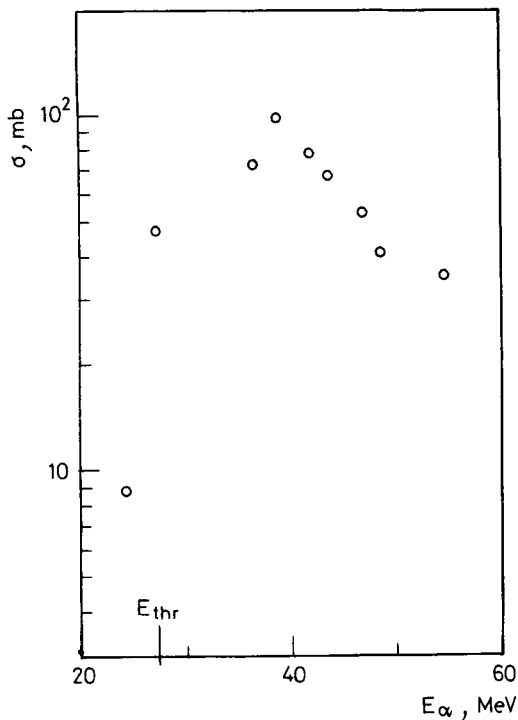


Fig. 5. Excitation function for the $^{103}\text{Rh}/\alpha, \alpha 3n/^{100}\text{Rh}$ reaction

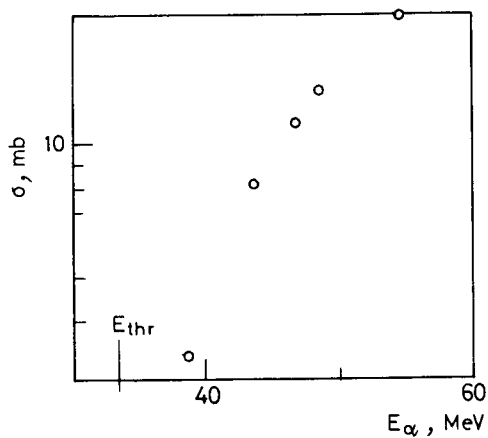


Fig. 6. Excitation function for the $^{103}\text{Rh}/\alpha, \alpha 4n/^{99m}\text{Rh}$ reaction

TABLE 3

Energy range /MeV	Thickness of the target / $\frac{mg}{cm^2}$	Cross-section /mb/	Saturation activities / $\mu Ci/\mu A/$	Σ Saturation activity / $\mu Ci/\mu A/$	$\Sigma A_t/10$ / $\mu Ci/\mu A/$	ΣA_h / $\mu Ci/\mu A/$
16-18	1.20	40	2.3904×10^2	2.3904×10^2	1.6007×10	1.6832×10^1
18-20	1.30	355	2.2811×10^3	2.5202×10^3	1.6877×10^2	1.7746×10^0
20-22	1.38	530	3.6205×10^3	6.1407×10^3	4.1122×10^2	4.3241×10^0
22-24	1.48	680	4.9746×10^3	1.1115×10^4	7.4436×10^2	7.8720×10^0
24-26	1.56	825	6.3615×10^3	1.7476×10^4	1.1703×10^3	1.2306×10^1
26-28	1.64	895	7.2553×10^3	2.4732×10^4	1.6562×10^3	1.7415×10^1
28-30	1.72	795	6.7580×10^3	3.1491×10^4	2.1088×10^3	2.2175×10^1
30-32	1.80	550	4.8935×10^3	3.6384×10^4	2.4365×10^3	2.5621×10^1
32-34	1.89	360	3.3631×10^3	3.9748×10^4	2.6618×10^3	2.7989×10^1
34-36	1.96	250	2.4220×10^3	4.2170×10^4	2.8240×10^3	2.9694×10^1
36-38	2.04	170	1.7142×10^3	4.3884×10^4	2.9388×10^3	3.0901×10^1
38-40	2.11	120	1.2515×10^3	4.5135×10^4	3.0226×10^3	3.1783×10^1
40-42	2.19	100	1.0825×10^3	4.6218×10^4	3.0951×10^3	3.2545×10^1
42-44	2.27	85	9.5374×10^2	4.7172×10^4	3.1589×10^3	3.3217×10^1
44-46	2.34	75	8.6749×10^2	4.8039×10^4	3.2170×10^3	3.3828×10^1
46-48	2.41	65	7.7431×10^2	4.8813×10^4	3.2689×10^3	3.4373×10^1
48-50	2.49	55	6.7693×10^2	4.9490×10^4	3.3142×10^3	3.4849×10^1
50-52	2.52	45	5.6077×10^2	5.0051×10^4	3.3518×10^3	3.5244×10^1
52-54	2.52	35	4.3616×10^2	5.0487×10^4	3.3810×10^3	3.5551×10^1
54-56	2.82	60	8.3835×10^2	5.1326×10^4	3.4371×10^3	3.6142×10^1

TABLE 4

Energy range /MeV/	Thickness of the target / $\frac{mg}{cm^2}$ /	Cross section /mb/	Saturation activities / $\mu Ci/\mu A/$	Σ Saturation activity / $\mu Ci/\mu A/$	$\Sigma A_t/10$ / $\mu Ci/\mu A/$	ΣA_{th} / $\mu Ci/\mu A/$
8-10	0.82	6.5	2.6570x10	2.6570x10	1.7793	9.0128x10 ⁻²
10-12	0.92	7.5	3.4328x10	6.0899x10	4.0782	2.0657x10 ⁻¹
12-14	1.02	8.5	4.2981x10	1.0388x10 ²	6.9566	3.5236x10 ⁻¹
14-16	1.11	10.5	5.8025x10	1.6190x10 ²	1.0842x10	5.4918x10 ¹
16-18	1.20	14.5	8.6652x10	2.4856x10 ²	1.6645x10	8.4310x10 ⁻¹
18-20	1.30	26.5	1.7028x10 ²	4.1884x10 ²	2.8048x10	1.4207
20-22	1.38	50.0	3.4155x10 ²	7.6040x10 ²	5.0922x10	2.5792
22-24	1.48	75.0	5.4867x10 ²	1.3090x10 ³	8.7664x10	4.4403
24-26	1.56	82.5	6.3615x10 ²	1.9452x10 ³	1.3026x10 ²	6.5981
26-28	1.64	81.0	6.5662x10 ²	2.6018x10 ³	1.7423x10 ²	8.8254
28-30	1.72	70.5	5.9938x10 ²	3.2012x10 ³	2.1437x10 ²	1.0858x10
30-32	1.80	55.0	4.8935x10 ²	3.6905x10 ³	2.4714x10 ²	1.2518x10
32-34	1.89	37.0	3.4566x10 ²	4.0362x10 ³	2.7029x10 ²	1.3690x10
34-36	1.96	25.0	2.4220x10 ²	4.2784x10 ³	2.8651x10 ²	1.4512x10
36-38	2.04	16.0	1.6133x10 ²	4.4398x10 ³	2.9732x10 ²	1.5059x10
38-40	2.11	12.0	1.2515x10 ²	4.5649x10 ³	3.0570x10 ²	1.5484x10
40-42	2.19	9.0	9.7425x10	4.6623x10 ³	3.1222x10 ²	1.5814x10
42-44	2.27	8.0	8.9764x10	4.7521x10 ³	3.1823x10 ²	1.6119x10
44-46	2.34	7.0	8.0965x10	4.8331x10 ³	3.2365x10 ²	1.6393x10
46-48	2.41	6.5	7.7431x10	4.9105x10 ³	3.2884x10 ²	1.6656x10
48-50	2.49	6.0	7.3847x10	4.9843x10 ³	3.3378x10 ²	1.6906x10
50-52	2.52	6.0	7.4770x10	5.0591x10 ³	3.3879x10 ²	1.7160x10
52-54	2.52	6.0	7.4770x10	5.1339x10 ³	3.4380x10 ²	1.7414x10
54-56	2.82	6.0	8.3835x10	5.2177x10 ³	3.4941x10 ²	1.7698x10

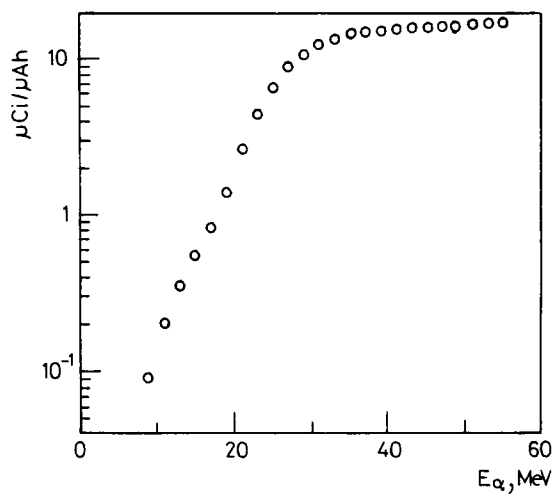


Fig. 7. Thick-target yields for the $^{105}\text{g}_{\text{Ag}}$ production

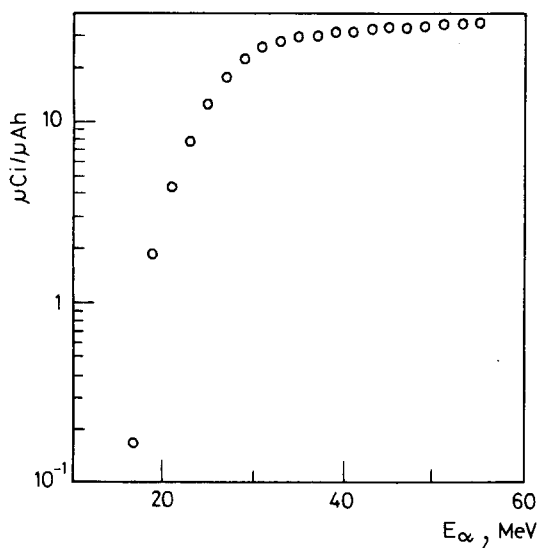


Fig. 8. Thick-target yields for the $^{106}\text{g}_{\text{Ag}}$ production

The thick target yields for ^{105g}Ag and ^{106m}Ag production were calculated by numerical integration applying experimental cross-section values obtained in the present work /Figs 1 and 2/, into Münzel and Svoboda's method^{18,19}. A computer program²⁰ was developed.

Values for energy integration ranges are listed in Tables 3 and 4. Our results are shown as plots of yields vs. α -particle energy in Figs 7 and 8.

*

The authors are indebted to the Synchrocyclotron staff who performed the irradiations.

REFERENCES

1. H.L. Brandt, D.J. Tendam, Phys. Rev., 72 /1947/ 1117.
2. I.de Betancourt, S.J. Nassiff, Radiochim. Acta, 12 /1969/ 206.
3. L.N. Siri, S.J. Nassiff, Radiochim. Acta, 14 /1970/ 159.
4. S.J. Nassiff, H. Münzel, Radiochem. Radioanal. Lett., 12 /1972/ 353.
5. S.J. Nassiff, H. Münzel, Radiochim. Acta, 19 /1973/ 97.
6. M.E. Lalli, C. Wasilevsky, O.R. Herreros, S.J. Nassiff, Radiochim. Acta, 23 /1976/ 107.
7. N.T. Porile, D.L. Morrison, Phys. Rev., 116 /1959/ 1193.
8. STOPY /unpublished/.
9. C.F. Williamson, J.P. Boujot, J. Picard, Tables of Range and Stopping Power of Chemical Elements for Charged Particles of Energy 0.05 to 500 MeV. Report C.E.A.-R-3042, 1966.

10. P.A. Baedeker, Anal. Chem., 43 /1971/ 409.
11. S. Taczanowsky, Precision of Direct Methods of Photo-peak Integration in Cases of Sloping Background. I.T.J. No. 37/I, 1973.
12. Unpublished.
13. FITEO /unpublished/.
14. Nuclear Data Sheets, National Academy of Sciences, Vol. 13, No. 3, November 1974, and Vol. 18, No. 2. June 1976.
15. G. Ertmann, W. Soyka, Die Gamma-Linien der Radionuklide. Jül-1003-AC, 1973.
16. L.F. Hansen, M.L. Stelts, Phys. Rev., 136 /1964/ 1000.
17. K.A. Keller, J. Lange, H. Münzel, Landolt-Börnstein, Numerical Data and Functional Relationships in Science and Technology, Vol. 5, Part a /1973/, Part b /1973/, Part c /1974/.
18. J. Lange, H. Münzel, Abschätzung unbekannter Anregungsfunktionen für $/\alpha, xn/$, $/\alpha, pxn/$, $/d, xn/$, $/d, pxn/$ und $/p, xn/$ Reaktionen. KFK-767, 1968.
19. K. Svoboda, On Terms Used in the Production of Radioisotopes by Charged Particle Bombardment. U.J.V. Report 2258. Ch. Czechoslovakia, 1969.
20. I. Dicke /unpublished/.